Copper electrodeposits in paper support

D. B. Hibbert
Department of Analytical Chemistry, University of New South Wales, P.O. Box 1, Kensington, Sydney 2033, Australia

J. R. Melrose*
Department of Chemistry, Royal Holloway and Bedford New College, Egham, Surrey, TW20 0EX, United Kingdom
(Received 3 November 1987)

Copper electrodeposits from an acid solution were grown, supported by laboratory filter paper. The paper provides good sample preservation and prevents convective solvent motion. Structural data from electron microscope and image analysis are reported. On decreasing the applied voltage, a transition from dense radial growth to open growth was observed. Values of the fractal dimension measured by image analysis for a series of growths were found in the range 2.0–1.7. The growths were often inhomogeneous and anisotropic, both on the microscopic and macroscopic scales. A number of growths were not fully characterized on the macroscopic scale by a single value to the fractal dimension. Wide variation in the microstructure of the growths was observed. On the micrometer scale, irregular microcrystalline, dendritic microcrystalline, and granular deposits were found. Copper surface densities were measured by x-ray microanalysis; fractal interpretations of observed scaling in these data were found to be unsatisfactory.

I. INTRODUCTION

Recently several authors[1–5] have investigated the growth of electrodeposited metals with emphasis on regimes characterized by fractal geometry[6,7] and dendritic growth.[8] Following the investigation[1] of copper electrodeposits in a spherical geometry, we report here copper electrodeposition in a planar geometry: solution-damp standard laboratory filter paper.

The use of a support medium facilitates electron microscope investigations, aids subsequent experimentation, and gives good sample preservation. Support of the tenuous growths would be a basic requirement for possible experiments in electrocatalysis. In addition, the study of diffusion-controlled growth within a porous medium (which we assume to be nonfractal) may be of relevance to problems of fluid displacement within a porous medium and dielectric breakdown.[9] However, the support media were often found to bring the penalty of inhomogeneous and anisotropic growth. The filter paper damps out convective solvent motion; it is used in electrophoresis techniques[10] for this very purpose.

The aim of the present work is to introduce the experimental technique and to report structural data gathered by image analysis and electron microscope observations. Section II describes some experimental details. Section III discusses image analysis and macroscopic observations. Section IV presents electron microscope observations. Section V discusses some x-ray microanalysis of copper surface density. Section VI brings discussion and conclusions.

II. EXPERIMENTAL DETAILS

A. Apparatus

The experimental setup involved a hardened filter paper (Whatmann 542, 541, and 540). A copper ring anode of internal diameter 8 cm, external diameter 9.5 cm, and thickness 0.5 mm was clamped on top of the paper, and the tip of a copper wire was placed central to the anode to act as the cathode and center of growth. The filter paper was in contact at the anode with a reservoir of the solution via more filter paper. A Plexiglas sheet was used to encase the growth region to prevent evaporation effects. A potentiostat (Thompson Associates Ministat) was employed to keep the cathode at a constant potential with respect to a reference potential. The chosen reference was a copper electrode in a bath of the experimental solution in capillary contact with the paper surface. As opposed to the standard technique, the reference electrode capillary contact cannot, due to the growth, be maintained close to the deposition surface. Instead, the capillary contact was made on the paper 5 mm in from the inner edge of the anode; this introduces the complication of "iR" drop[11] across the paper varying as the growth approaches the capillary contact point. In addition, the growths themselves were found to have significant resistance. For these reasons, growth potentials quoted in this work are not the overpotential at the growing interface and are specific to the particular experimental arrangement. Some details of these effects are given later in this section. The potential of the copper reference electrode was measured, in the experimental

solution (0.75 mol dm^{-3} $CuSo_4$, 1 mol dm^{-3} H_2SO_4), against a saturated KCl calomel electrode, and found to have a value of 0.27 V with respect to the standard hydrogen electrode. Potentials below are quoted with respect to the copper reference electrode. Potentiostatic voltages in the range 0.4–3.0 V were applied. In addition, several growths were made without the potentiostat in the range 1.0–25 V applied directly between the anode and cathode.

Image analysis of 704 × 896 bit maps were carried out on a Cambridge Instruments Quantimet 970 under QUIPS software. Electron microscope investigations were carried out on a Cambridge Instruments S100 SEM and LINK systems EDX.

B. Solutions and paper

In the preliminary experiments, several aqueous solutions were investigated: (a) 0.01 mol dm^{-3} $CuSo_4$, 0.5 mol dm^{-3} Na_2SO_4 (Ref. 1) (measured *p*H 5.03); (b) 0.1 mol dm^{-3} $CuSO_4$, 0.1 mol dm^{-3} Na_2SO_4 (measured *p*H 4.4); (c) 0.1 mol dm^{-3} $CuSO_4$ (measured *p*H 4.3); (d) 0.5 mol dm^{-3} $CuSO_4$ (measured *p*H 3.1); and (e) (from 0.75 mol dm^{-3} to 0.1 mol dm^{-3}) $CuSO_4$ in 1 mol dm^{-3} H_2SO_4 (measured *p*H 0.0). The result of using solutions (a), (b), and (c) was simply a blue ring around the cathode. Only growth from solutions (d) and (e) was successful. The best results (with respect to macroscopic size) were achieved with the acid solutions (e). In the present work, results for solutions (e) (and in the main for 0.75 mol dm^{-3} $CuSO_4$) are presented. An attempt to grow from a $CuSO_4$ solution in the organic solvent acetonitrile was unsuccessful.

A systematic investigation of solutions with respect to the success or otherwise of growth was not pursued. The cellulose fibers of the paper have carboxyl groups (—COOH) on their surface which will begin to be ionized as the carboxylate anion in solutions of *p*H greater than 2.0–3.0[10]. In high-enough *p*H, electroendosmosis[10] will result in fluid motion towards the cathode, enhancing cation migration in the many capillaries between the fibers. The absence of growth in the solutions (a)–(c) may result from these *p*H effects; however, the underlying mechanism is unclear. Copper growth does occur from solutions of Na_2SO_4 and $CuSO_4$ in the absence of cellulose fibers.[1] The *p*H of the solutions (e) should imply uncharged fibers and eliminate electroendosmosis in the cellulose medium. A complication arising from the use of acid solutions at the applied potentials is the presence of gas evolution at the growing interface.

For the three filter papers used, Whatmann 540, 541, and 542, no systematic variation in growth macrostructure was observed. It is noted that filter papers are designed for different flow properties through the plane of the paper rather than in the plane as of interest here. However, the different papers did possess different conductances when solution damp.

Unless otherwise stated, all growths reported below were made on Whatmann 541 paper damp with a 0.75 mol dym^{-3} $CuSO_4$, 1 mol dm^{-3} H_2SO_4 solution. A few growths were made in glass fiber paper; these will be mentioned briefly.

C. Growth conditions

The deposition of copper from acid solutions has been studied by several authors, Hibbert *et al.*[12] and references therein. The reaction kinetics obeys the following scheme:

$$Cu^{2+}(aq)+e^- \mapsto Cu^+(\text{surface}) ,$$

$$Cu^+(\text{surf})+e^- \mapsto Cu ,$$

with the first step being rate limiting. The experimental solutions were of *p* H 0.0, which gives an equilibrium potential for the hydrogen electrode reaction, of −0.27 V (versus Cu reference electrode). Thus at potentials less than −0.27 V, hydrogen may be evolved. The presence of hydrogen evolution was confirmed by the addition of a few drops of H_2SO_4 onto the growing tips and the observation of a current increase, and found present down to the lowest applied voltages (0.4–0.6 V).

During growth, concentration gradients in Cu^{2+} ions were observed. The interior and regions around the growths were observed to be devoid of the characteristic blue color of hydrated Cu^{2+} ions. These color changes were enhanced by holding the fresh growths over a beaker of concentrated ammonia solution. The regions devoid of blue color extended some 0.2 to 1.0 cm beyond the growth radius for 3.0 to 1.0-V growths, respectively. Cu^+ is absent in the acid solutions. With the hydrogen ions dominating conduction and the presence of large concentration gradients in Cu^{2+} around the growth, we believe that, at least at the lower applied voltages, the transport of Cu^{2+} to the growing interface was diffusion controlled. However, despite the absence of convection currents, the electric field is probably not screened from the solution. The hydrogen ions are reduced at the cathode, and the current of sulphate ions is assumed balanced by the presence of the reservoir. The cell itself possessed a current proportional to voltage. This, we believe, is mainly due to hydrogen evolution which is limited by proton migration in the resistive paper medium.

The experimental setup, with the reference electrode some 3.5 cm from the central cathode, introduces problems of control. At any time during growth, the potential across the growing interface is reduced from that set at the potentiostat by the potential drop across the growth itself, a concentration overpotential,[11] and the potential drop between the radius at the capillary contact point of the reference electrode and the interface, the latter potential drop being given by the finite resistance of the solution damp paper and the current passed at that time. Measurements using a standard ac conductance bridge gave resistances on Whatmann 541 paper between the cathode and anode prior to growth in the range 300–500 ohm. The paper conductance varies with the dampness of the paper, necessitating the blotting of the paper prior to growth. By use of copper probe rings, it was found that disks of the paper containing a growth possessed a center to perimeter resistance in the range 50–70% of control damp paper disk resistances; hence the net resistance falls during growth. Current time graphs, although often not smooth, showed an $I \propto t^{\alpha}$ behavior, with α in the range 0.2–0.5. Figure 1 shows a typical result.

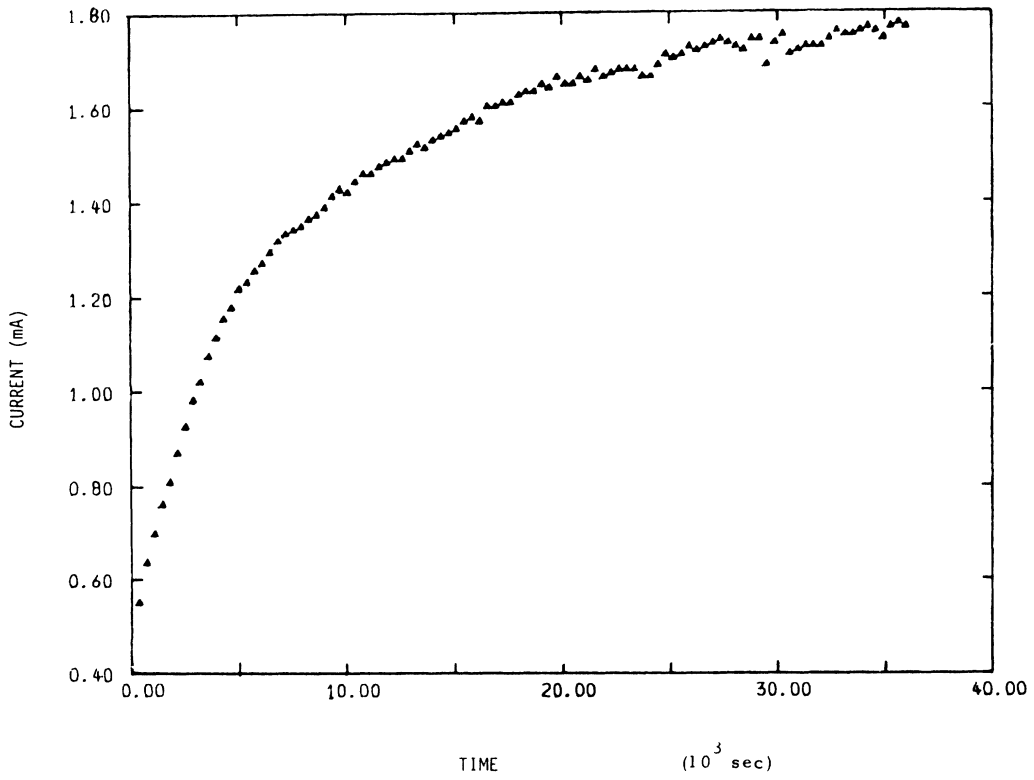

(25)

FIG. 1. Measured current against time for a 1-V potentiostatic growth from 0.75 mol dm^{-3} $CuSO_4$, 1 mol dm^{-3} H_2SO_4.

Current increases from beginning to end of growth varied from a 0.1- to 0.3-mA increase for a 2.5-cm-diam 0.5-V growth to a 2.0- to 21.0-mA increase for a 3-cm-diam 3-V growth. Although the net resistance falls, the "iR" drop will increase with the current. We suspect that, after the initial stages of growth, the potential drop at the interface will decrease from an initial value reduced from that applied. For a 0.8-V (potentiostatically applied) 3-cm growth, we estimate from crude measurements an initial interface potential drop of 0.5 V decreasing to 0.35 V by the end of growth. However, the logarithmic dependence on radius of the center to perimeter resistance of a disk and the observed current variation implies that the largest variation of interface potential will occur during the initial stages of growth. A number of experimental problems have prevented accurate measurement of these effects. In any case, characterization of the growing interface as an equipotential is problematical given the resistive character of the growth, variable microstructure, and tree geometry. Growth from applied potentials below 0.4 V was not observed. A description of growth conditions on the microscopic scale is given in Sec. IV. Growth times varied from 60 h for a 2.5-cm-diam growth at 0.5 V, through 15 h for a 4.5-cm-diam growth at 0.8 V, to 5 h for a 4.5-cm-diam growth at 2.8 V.

III. MACROSTRUCTURE AND IMAGE ANALYSIS

A number of growths were grown potentiostatically in the potential range 0.4–3.0 V from a 0.75 mol dm^{-3} $CuSO_4$, 1.0 mol dm^{-3} H_2SO_4 solution. Figure 2 shows photographs of five of these growths. With increasing voltage a trend from open growth to dense radial growth with circular outer envelope is clearly seen. In nonpotentiostatic deposition zinc experiments,[3,4] on increasing voltage, regimes of open, dense radial, dendritic, and finally, stringy growth morphologies were identified. The presence of convection currents in the zinc experiments leads to the conclusion that the electric field is not screened within the cell and that growth is governed by the electrostatic analog of diffusion-limited aggregation (DLA).[3,4,13] To allow more direct comparison with the zinc experiments, we grew copper from the acid solutions without potentiostatic control both with paper support and without support confined between two Plexiglas disks.[4] The supported growths showed a steady transition from an open branched to dense radial pattern up to the highest applied voltage of 25 V; no regime of dendritic or stringy[3,4] growth was found. As in the zinc experiments, lowering the $CuSO_4$ concentration at a given voltage brought a more open structure. In sharp contrast, over the 1–25 V range studied, the unsupported growth was entirely of a stringy morphology, accompanied with vigorous gas evolution and rapid in comparison to the growth within support (of the order of minutes rather than hours).

Image analysis was pursued on the potentiostatically grown samples. Fractal dimensions, d_f were measured using area radius scaling.[14] Some 13 origins on the image were chosen and, for some 20 circles of increasing radii r, enclosed detected areas were averaged over the origins. Least-squares fits to $\ln(\mathbf{r})$ against $\ln(\langle A(r)\rangle)$ gave d_f. A

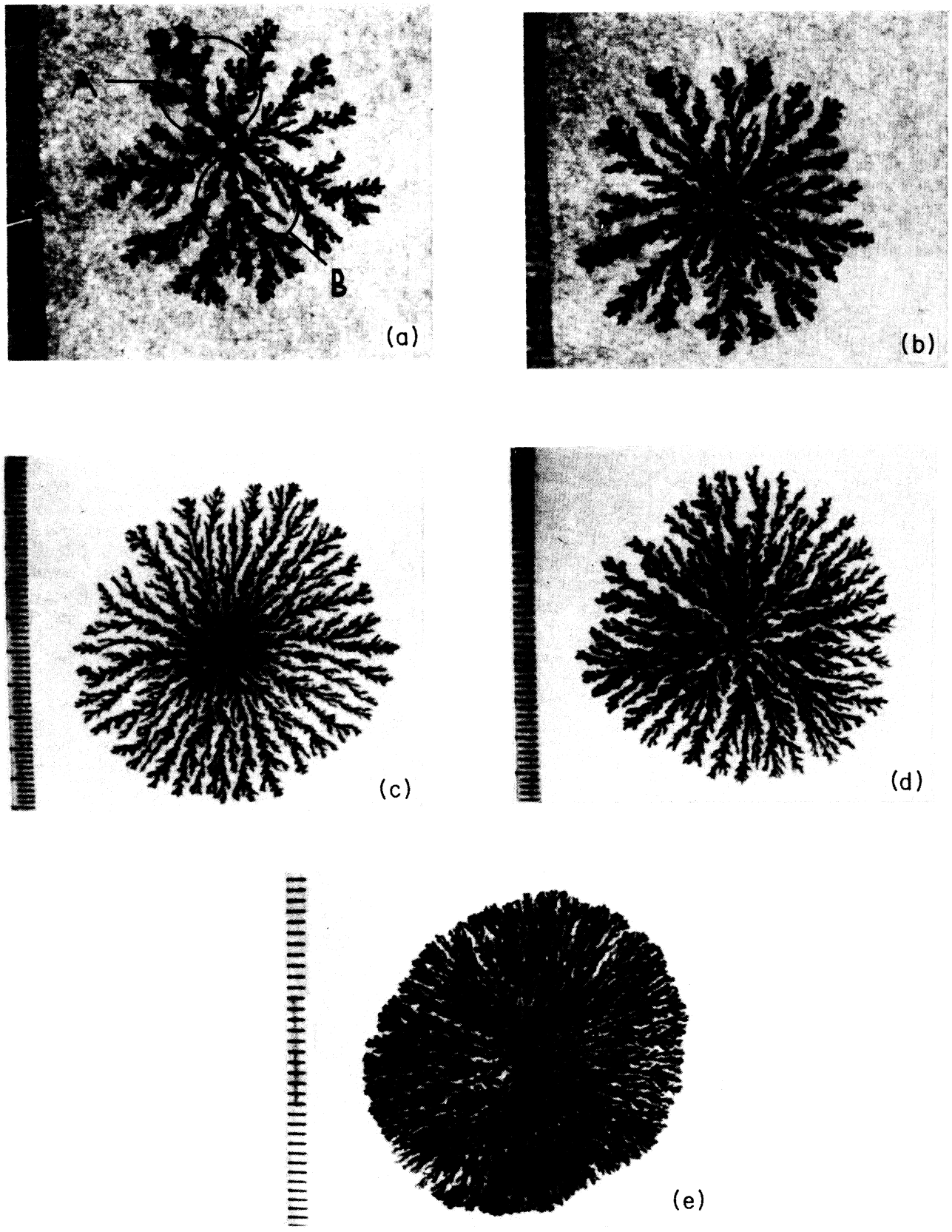

FIG. 2. Five samples grown potentiostatically from 0.75 mol dm^{-3} $CuSO_4$, 1 mol dm^{-3} H_2SO_4. (a) 0.5 V, d_f varying from 1.73 in region A to 1.91 in region B. (b) 0.7 V, $d_f = 1.79$. (c) 0.8 V, $d_f = 1.86$. (d) 1.6 V, $d_f = 1.95$. (e) 3 V, $d_f = 1.99$. A mm scale is shown.

fresh bit map was made at each detection. Care was taken to avoid dense center and growing interface errors. The higher moments,[14]

$$D_q = \frac{1}{q} \frac{d\ln(\langle a(L)^q \rangle)}{d\ln(L)} , \quad (1)$$

for $q=2$ and 3 were also measured; $d_f = D_1$. Several d_f values so obtained were averaged to allow error estimates.

Figure 3 shows values of d_f against growth voltage for several growths satisfying criteria of homogeneity (see below). Values of d_f approach the diffusion-limited aggregation value,[15,16] 1.71, at low voltage and show a noisy increase to 2 with voltage. The noisy data reflect the difficulties of experimental control of the supported growth conditions. The question of a sharp transition in d_f is not resolved by the data. The bound $d_f < D_2 < D_3$ was found on all samples studied; however, differences between the D_q were only of the order 0.1% to 0.5% of d_f.

Growths were often anisotropic and inhomogeneous. Figure 4 shows some examples and Fig. 2(a) another. Often, different regions of the same growth possessed different fractal dimensions over the mm to cm scale. Figures 4(a), 4(b), and 2(a) give examples of this. Figure 5 shows area scaling results from two different regions of Fig. 2(a). The samples whose d_f values are reported in Fig. 3 were deemed homogeneous in that regional variations in d_f above the inherent inaccuracy were not detected.

The sensitivity of growth morphology to lattice symmetry and sticking probability in lattice simulations[15,17] is well known. Here, however, the growth morphology is probably coupled to more external anisotropies and inhomogeneities. In a number of cases, anisotropies in the experimental setup were found. In particular, anisotropies in the flux of new solution from the reservoir correlated with growth anisotropies. Degradation of the anode was another cause. Centering of the cathode was found not to be critical (in the disk geometry, resistive effects are relatively insensitive to cathode location). While setting the cathode off center, up to 1–2 cm, was capable of producing anisotropy (the more so the lower the voltage), this often was not to the same degree found in carefully centered samples. Distortion of the cathode tip did not correlate with anisotropies. Many cases defied obvious explanation. It is plausible that the filter paper can support anisotropic fluctuations in the copper flux resulting from external variations at the anode reservoir contact or from inhomogeneities, such as fiber density, in the paper itself. As will be shown in Sec. IV, the fiber environment can, on the 100-μm scale, induce branching additional to that inherent in the growth scenario. Hence branching rates and branching angles on the mm scale under observation by the image analyzer may be both artificial with respect to that found in the absence of media and sensitive to paper inhomogeneities. In addition, different rates of hydrogen evolution and copper deposition, due to potential variations, may couple to the anisotropies.

Inhomogeneities were reported in the zinc experi-

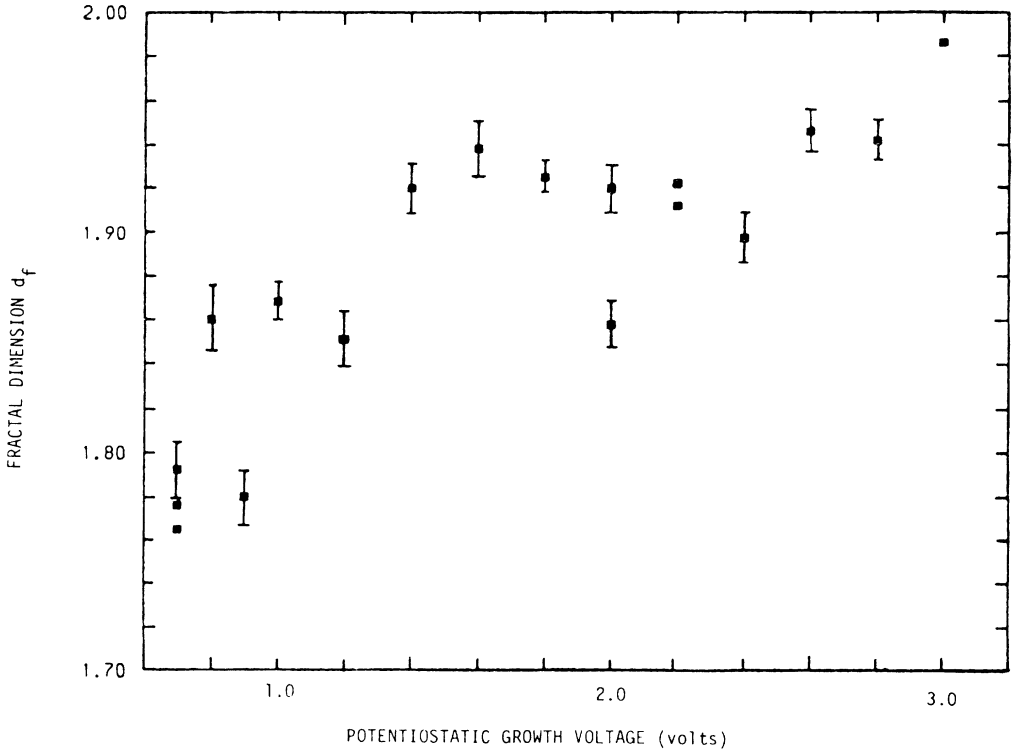

FIG. 3. Values for d_f against potentiostatic growth voltage; error bars are shown.

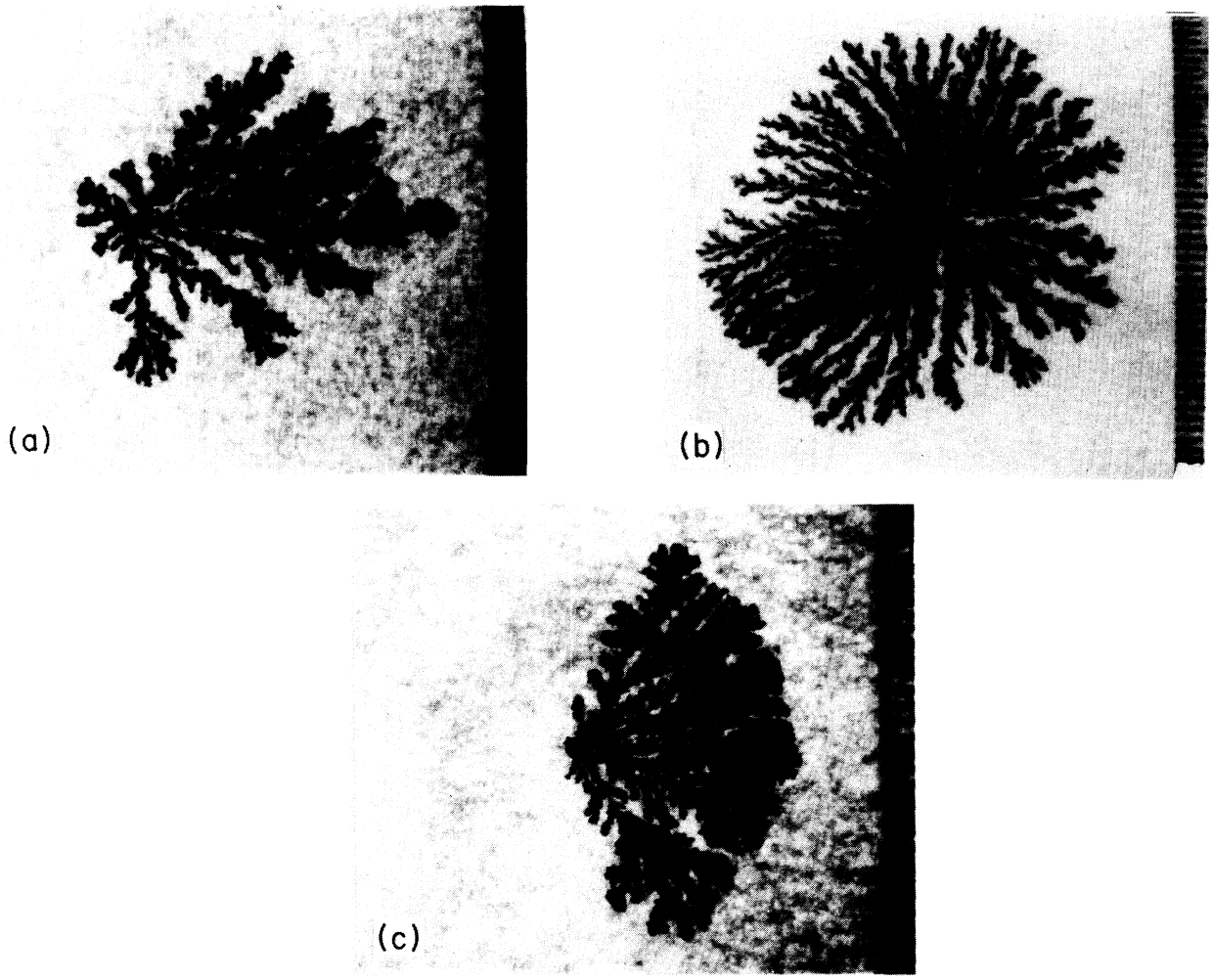

FIG. 4. Three samples showing anisotropic and inhomogeneous growth. (a) 1 V, (b) 1.4 V, and (c) 1 V. A mm scale is shown.

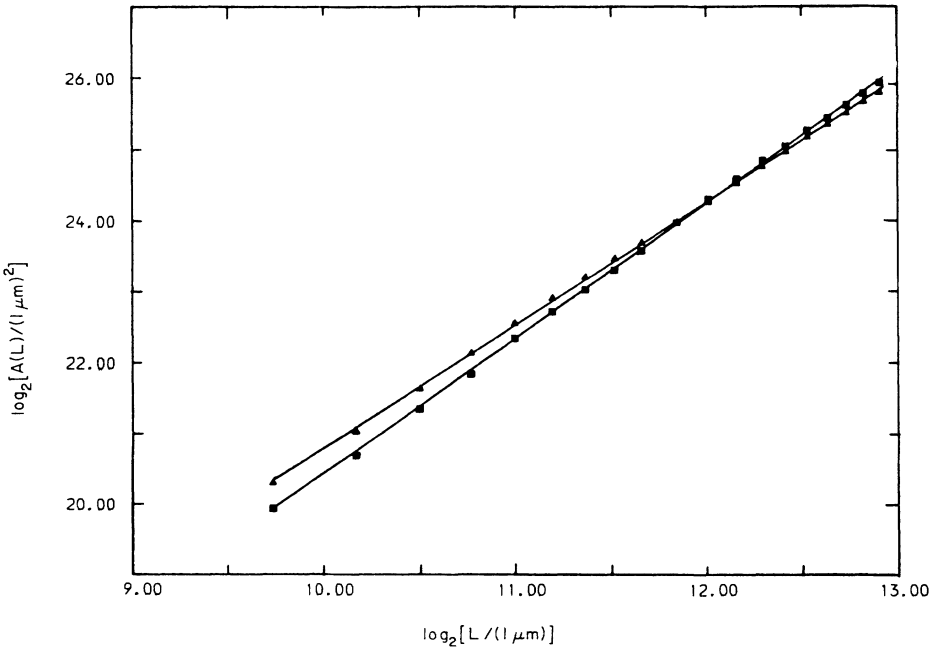

FIG. 5. Plots of $\log_2$ (detected area) vs $\log_2$ (radius) measured in two regions of the Fig. 2(a) sample. Closed triangles, region A ($d_f = 1.73$), closed squares, region B ($d_f = 1.90$).

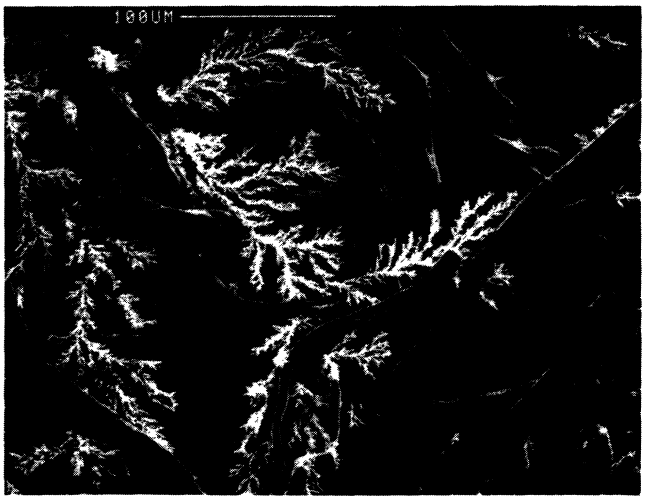

(a)

(b)

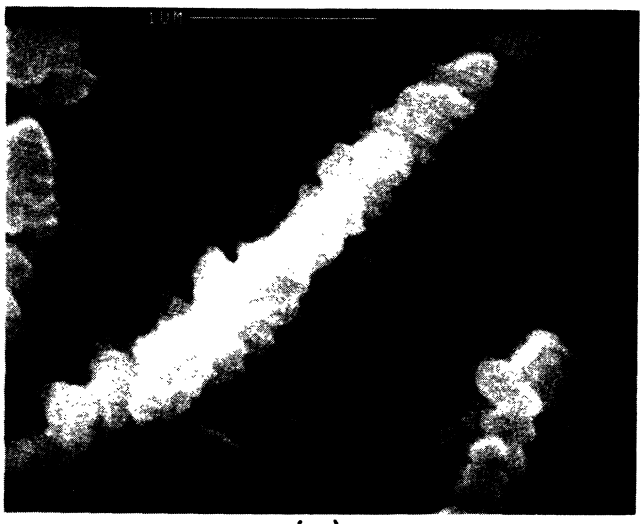

(c)

FIG. 6. Electron micrographs of the same region at three different magnifications from a growth at 1 V from a 0.25 mol dm^{-3} $CuSO_4$, 1 mol dm^{-3} H_2SO_4 solution. The growth in (a) is that which is central in (b). The white square in (b) indicates the dendrite shown in (c).

ments.[3,4] A circularly symmetric crossover from open to dense radial growth was observed during the initial stages (0.5 cm) of growth. Particularly for high-voltage (8–20 V) nonpotentiostatic growths, similar effects were observed in the present experiments. One possible explanation lies in the variation of potential drop at the interface due to resistive effects. As discussed in Sec. I, this should be greatest in the initial stages of growth.

IV. MICROSTRUCTURE

Some 15 samples were studied on the SEM: grown nonpotentiostatically (3–15 V) and potentiostatically (0.4, 0.5, 1.0, and 2.0 V), samples at different $CuSO_4$ concentrations, a growth in glass fiber paper, and a small deposit from a nonacid solution [(d) of Sec. II)]. Several of the electron micrographs taken of the potentiostatically grown samples are shown in Figs. 6–12. These will be

(a)

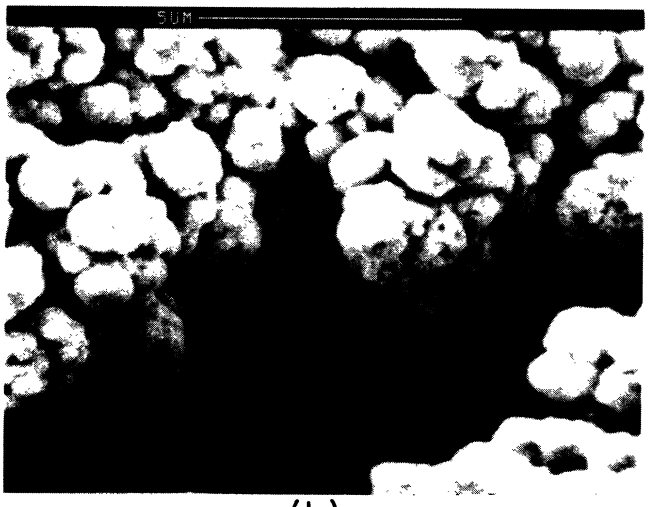

(b)

FIG. 7. The same region at two different magnifications from a growth at 2 V from 0.75 mol dm^{-3} $CuSO_4$, 1 mol dm^{-3} H_2SO_4. (b) is a close-up of the trough that is central on the growth of (a).

used to illustrate discussion of growth microstructure. Micrographs of the same region at different magnifications are presented in the same figure.

The paper consists of a mat approximately 0.2–0.5 mm thick, of cellulose fibers approximately 10–20 μm in diameter [see Figs. 6(a), 7(a), 8, and 9(a)]. Cellulose sheets and fine micrometer-diameter cellulose filaments were also present. Most of the micrographs reveal features appearing within the rough surface of the mat. (The division of the mats into surface and interior is somewhat artificial, the surface roughness being of the order of the mat thickness.) Observations of a soaked mat of string and optical microscope observations of the damp paper were made. We observed the fluid surface of a solution-damp mat to be one of water menisci suspended between and around the fibers by surface tension. The ion transport and growth takes place in fluids layers of varying thickness, the layers being found thicker as they curve up to the most protruding fibers and within pores dropping into the interior. The mobility of ions in the filter paper is known to be reduced roughly one half of that in pure solution.[10] This has been attributed to the effects of restrictive and tortuous paths.[10] Electroendosmosis is assumed absent (see Sec. I). We assume that the fluid environment described above does not constitute a fractal in itself.

Growth was observed on both surfaces of the paper; although, in general, one surface was consistently more covered than the other. Figure 9(a) shows a section along the growth direction of a major branch of a 0.4-V growth. Note in many respects that this growth is atypical.

Figures 6(a), 7(a), and 8 reveal that the fibers affect the progress of growth on the 100-μm to -mm scale. Clearly, in Fig. 6(a), the growth at the center has branched along water menisci suspended from the fiber barrier. Note that the branch angle is determined by the fiber barrier. At the top of Fig. 6(a) is an example where growth has followed a fluid-filled channel between two fibers. Such quasi-one-dimensional growths can often be found on the mat surface. However, growth does not occur directly on the fibers. Figure 8 clearly shows this. One reason for this may be that the fibers are sheathed in a water layer devoid of Cu^{2+} ions; a stationary water sheath may inhibit Cu^{2+} transport.

On scales between 0.5 and 5 μm, the growths become compact. With some degree of lattitude [particularly between categories (i) and (ii)], we classify the growth structures, on scales less than 10 μm, into three categories: (i) *Irregular microcrystalline* plate and needle shaped microcrystals of size 0.5 to 1.0 μm arranged irregularly on a branched structure, see Figs. 11(b), 8, and 12; (ii) *dendritic microcrystalline,* plate and needle microcrystals arranged in a typical dendrite tip and side branching structure,[8] see Figs. 6(c) and 10(b); (iii) *granular aggregates,* see Figs. 7(b) and 9(b); these resemble micrographs of the structure of copper deposits in a spherical geometry.[1,18] Although the different categories are evident on scales less than 10 μm, it should be noted that, to the eye, on

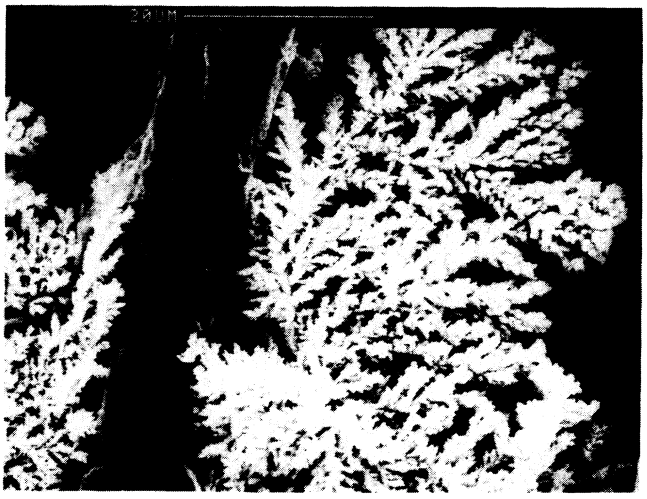

FIG. 8. A growth and fiber from a 3-V growth from 0.75 mol dm^{-3} $CuSO_4$, 1 mol dm^{-3} H_2SO_4. Note that the growth avoids the fiber surface.

(a)

(b)

FIG. 9. Two different magnifications from 0.4 V, 0.75 mol dm^{-3} $CuSO_4$, 1 mol dm^{-3} H_2SO_4.

(a)

(b)

FIG. 10. A growth from 2-V, 0.75 mol dm^{-3} $CuSO_4$, 1 mol dm^{-3} H_2SO_4 solution. The dendrites of (b) are central to (a). Note the tip splitting on the left-hand finger.

(a)

(b)

FIG. 11. A growth from 1 V, 0.5 mol dm^{-3} $CuSO_4$, 1 mol dm^{-3} H_2SO_4. The white square in (a) indicates the tip shown in (b).

the 50- to 100-μm scale, each growth sample was unique in form (compare Figs. 7 and 9 or Figs. 6 and 10). These microstructures are in sharp contrast to those found in copper deposition from acid solution onto single crystals.[19] In the latter experiments, terraced rough surfaces are observed and understood on the basis of terrace growth bunching and spiral terrace growth mechanisms.

Branching structures on the 100-μm scale can be formed from all three categories; see Figs. 6–12. Occasionally, dense unbranched regions of category-(iii) structure were found. Different categories were found on the same sample; Figs. 7 and 10 are from the same sample. Although the fibers can induce branching, branching is a feature of the growth both well below and well above the scale of the fibers.

From the few samples studied in the microscope, a clear systematic variation of growth structure with voltage cannot be deduced. The category-(i) and -(iii) structures were the most common, the dendrites being the rarest. Dendrites were found only on the 0.5-, 1.0-, and 2-V potentiostatically grown samples. The evidence supports the idea[3,4] that dendritic growth occurs in a narrow range of conditions. High-voltage growths consisted of both (i) and (iii) structures. A 0.4-V growth (see Fig. 9) was quite distinct, in that all branches were of granular deposits and had dimensions comprable to that of the fibers.

Figures 12, 6, and 11 show trees found on samples grown at 1 V, from respectively, 0.1 mol dm^{-3}, 0.25, mol dm^{-3}, and 0.5 mol dm^{-3} $CuSO_4$ in a 1 mol dm^{-3} H_2SO_4 solution. A variation of structure with concentration is evident. All three are microcrystalline with the crystallite size and branching rates increasing and decreasing, respectively, with increasing concentra-

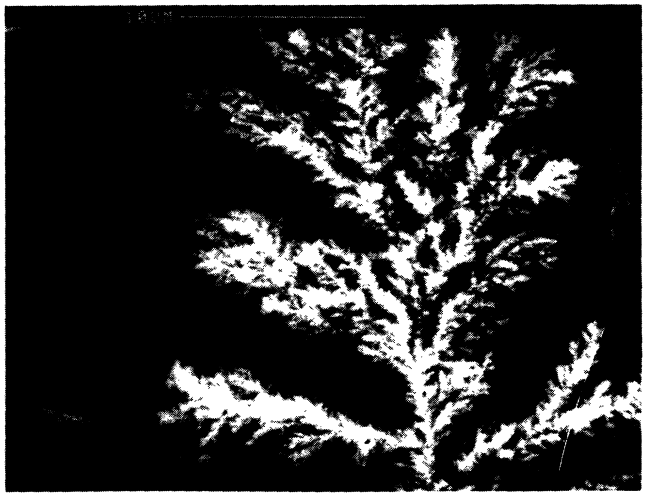

FIG. 12. A growth from 1 V, 0.1 mol dm^{-3} $CuSO_4$, 1 mol dm^{-3} H_2SO_4.

tion. Only the 0.25 mol dm^{-3} solution had a dendrite microstructure.

It is tempting to correlate the varying microstructure with the variation of fluid layer thickness between different locations on the mat, the thickness providing a length scale.[18] For DLA, three-dimensional (3D) transport supplying a deposit in 2D should result in a compact structure[13] on scales less than the layer thickness. The thick fingers of Fig. 7(a) presumably indicate the local fluid layer thickness. Particularly for high voltage growths, compact type-(iii) regions did correlate with high ridges on the mat surface. However, pores containing open branching dendrites [see Fig. 6(b)] and regions with evidence of dendritic growth at the bottom of fluid layers were also found. The form of growth in fluid layers of varying thickness is perhaps determined more by local transport and concentration fluctuations. However, assuming that the 0.4-V growth of Fig. 9 is close to the DLA limit, then its compact microstructure on scales comparable to the fluid layer may reflect the DLA causality bound.[13]

The two examples of dendrite regions, Figs. 6(c) and 10(b), both show paraboloidal tip and side branching features resembling experimental solidification dendrites and theoretical models thereof.[8] The ratio of the size of the spine to that of the side branches has a different value in the two examples. In the case of Figs. 6(c), the spine is a microcrystalline staircase. The left-hand branch in Fig. 10(b) appears to undergo a tip splitting instability. All dendrites were unstable with respect to tip splitting, which occurred every 5 to 20 μm.

Two of the growths studied were made within a glass fiber paper: a more open mat of 1- to 5-μm- thick fibers; and somewhat finer fibers than the cellulose paper fibers. The deposit was irregular microcrystalline. However, the microcrystals had smooth crystal facets and were of the order of 5 μm in scale, larger than those found in the cellulose paper. Samples grown in a $CuSO_4$ solution [(d) of Sec. II B)] in cellulose paper were of branched granular deposits with granules of the order of 0.1 μm scale and less, smaller than those found in the $CuSO_4$ and H_2SO_4 solutions. Clearly both fiber dimensions and hydrogen evolution (presumed less in the nonacid solution) influence the microstructure.

V. X-RAY MICROANALYSIS

Surface copper concentrations ρ were measured by the detection and counting of x-ray emissions in the channel corresponding to the copper K_α transition. The x-ray count averaged over several 100-s intervals is assumed to be proportional to the concentration of copper visible on the surface. Concentrations for a given region under a range of magnifications, M_1 to $M_{\max}$, were measured. Introducing a length scale via

$$L_i = \frac{M_{\max}}{M_i} ,$$

concentrations against length scales were obtained. Figure 13 shows the log-log plot of a typical result; a number of runs were made on a 2-V sample. Approximate length scales in mm are indicated. The regions were arranged with a growth central. Hence at the highest magnifications, the graph flattens out as the image is filled with copper. A scaling regime, $\rho \propto L^{\alpha}$, is observed at the shorter length scales, and values of α obtained where in the range -0.7 to -1.3. The scaling regime passes from length scales with single fibers in the image to length scales with many fibers in the image. Fractal explanations for this scaling are not appropriate: fitting to $\alpha = d_f - 2$ gives values of d_f unacceptably low for the DLA model. In the case of Fig. 13, this regime represents the crossover from a scale with just one growth in the image to a scale with a few separated growths in the image. Fits to the longer length scale results (see Fig. 13), when many growths were present in the image, gave values of d_f closer to those of the image analysis. However, data accuracy was poor at the longer length scales. On a different sample, regions containing trees fully connected throughout the low magnification image were studied; Fig. 14 shows a case with $\alpha = -0.17$. Another region from the same sample gave $\alpha = -0.5$.

VI. DISCUSSION AND CONCLUSIONS

The main emphasis of the present work is on the development of the technique of deposition within a support medium and the analysis thereof. Many of the results presented have hence been of an exploratory nature.

Copper electrodeposits were successfully grown from an acid solution within a paper medium. A number of higher-pH solutions with Na_2SO_4 as an indifferent supporting electrolyte were unsuccessful. The ionization of the carboxyl groups on the cellulose fibers above pH 2–3 may play a role in preventing growth.

The paper medium did provide a robust and preserving support and allowed ease of study under an electron microscope; samples were found to survive quite rough handling. We believe that, at least at low voltages, growth was diffusion controlled. Problems characterizing the

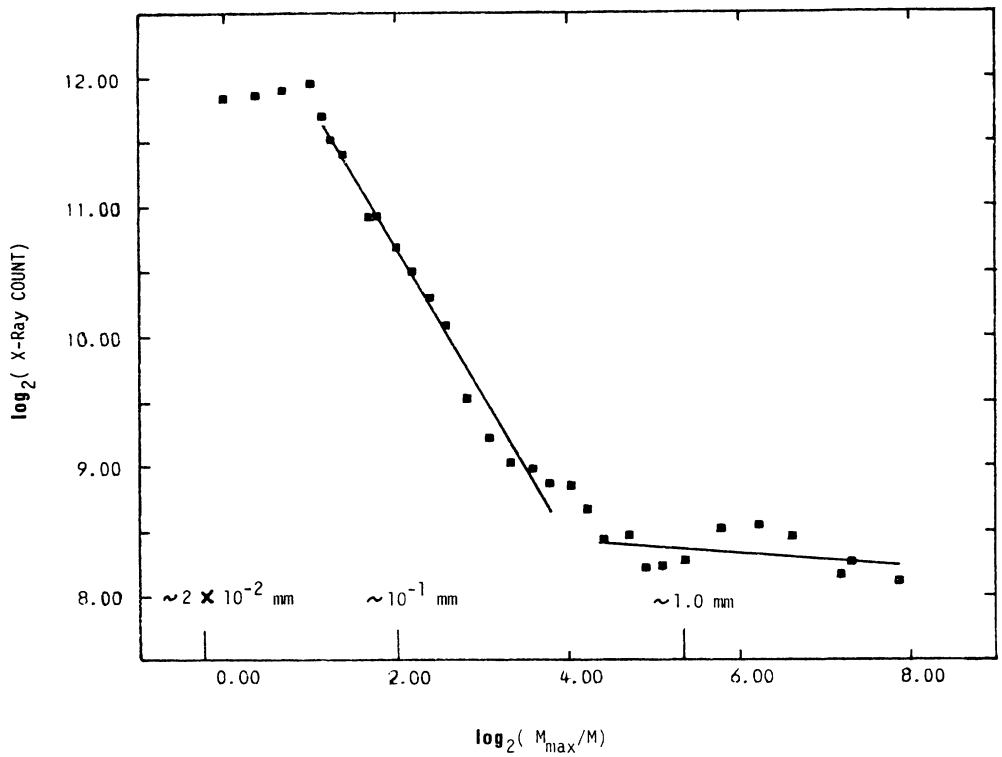

FIG. 13. Plot of $\log_2$ (x-ray emission count) vs $\log_2$ (M_{max}/M_i) (see text) for a region of a 2-V growth with many separate trees in the low magnification image. Approximate lengths in mm are indicated.

growth conditions, in particular, resistive effects and hydrogen evolution, need to be studied further. Other recent experiments[3,4] have also involved such problems.[5] The growths were not found to cling directly to the fibers; the fibers affected growth by forming barriers and channels and determining the fluid environment. Branching extended above and below the fiber scale. However, on the 100-μm scale, examples of fiber barriers inducing branching were found. Observed on the mm scale, branching rates and branch angles may well be artificial

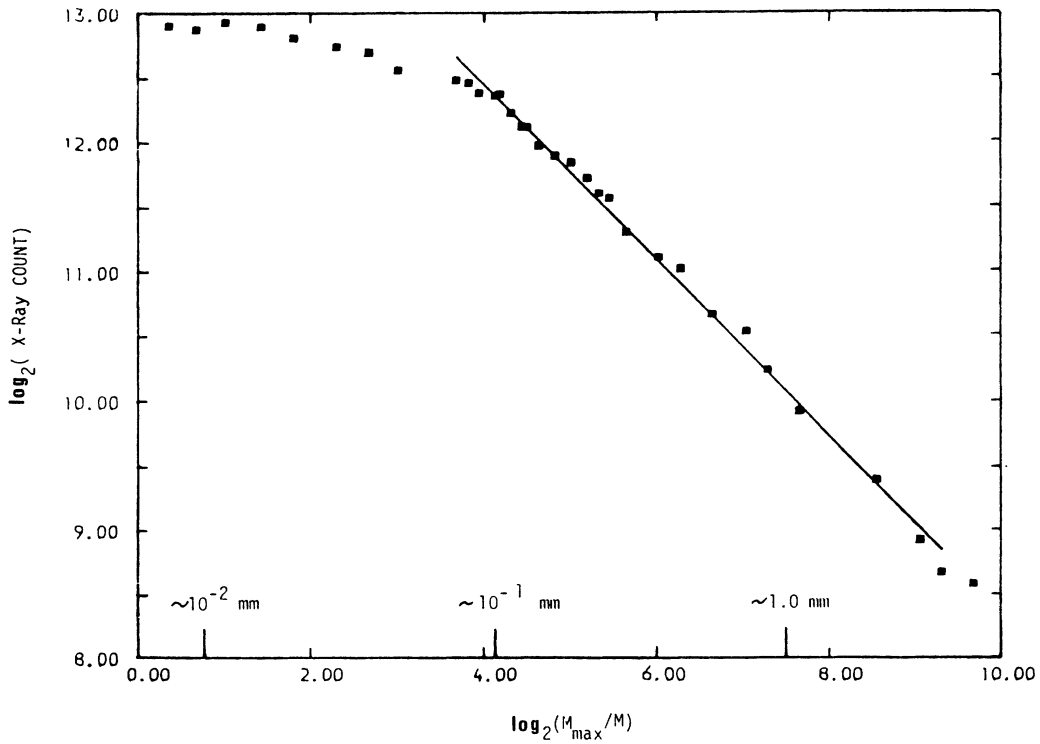

FIG. 14. Same as Fig. 13, but for a region of a nonpotentiostatic 3-V growth with a single tree in the low magnification image.

with respect to those expected for growth in the absence of support. For better interpretation of subsequent experiments, support media more homogeneous above the micrometer scale, such as gelatin, should be investigated. Growth in a glass fiber mat produced a radically different microstructure.

Once satisfactory control can be gained, a number of other experiments on preserved growths would be interesting; in particular, measurement of surface ac frequency response[20] and catalytic properties.[21] Much is known of the growth of single crystals. The understanding of the surface morphology of such crystals has made important contributions to our understanding of metal catalysts. However, in practice, such catalysts are often dispersed on a support. The morphology of growth found here is in sharp contrast to that observed for copper deposition on single crystals.[19] The more exotic and numerous growth forms here, with their connectivity and high surface area may offer catalytic advantages. However, restriction of chemical activity to just the outer perimeter of the growths is undesirable. To overcome this difficulty, we propose that growth may be made within a support medium in a cylindrical geometry (supported, for example, in silica gel columns). Reactants may then be admitted to the full surface area by passing them normal to the plane of growth.

A change from an open to a dense radial[3,22] macrostructure was observed on increasing the applied voltage. At low voltage, the fractal dimension of the open growths approached that of DLA. Direct comparison of the dense radial growths with computer simulations,[23] in particular, the presence of long channels and circular envelopes, would suggest that the dense radial pattern at high voltages is an example of unidirectional ballistic aggregation. An important question here is whether the dense radial pattern is a high-voltage regime of an electric field dominated transport, or whether it is characteristic of diffusion-controlled growth beyond the quasistationary regime[13] presently studied for DLA.[25] A relevant experiment on this question would be the use of time-lapse photography to observe growth radius against time. The appearance of stringy growth as an ultimate limiting form[3,4,34] at high voltage was found to be suppressed in the paper medium, while stringy growth was found to dominate growth in the experimental solution in the absence of a paper medium. On the basis of this observation, it is speculated that increased mass transport due to fluid motion (convection or gas agitation) enhances the stringy growth mode. A macroscopic dendrite regime was not observed, although a narrow regime of microscope dendrite growth was found. The growths were found to be very unstable with respect to anisotropy and inhomogeneity both in the experimental setup and, we believe, within the paper medium. A single value of fractal dimension was not sufficient, due to inhomogeneity, to describe mass scaling of many of the growths. Although some of the observed instability may be peculiar to electrodeposition, on the practical level this instability must suggest that media fluctuations may well dominate the analogous problems of fluid displacement and dielectric breakdown within media.

A number of questions concern the varied microstructure. Do the granular deposits have crystalline long-range order? What is the stability of the microstructures to changes in the applied conditions? One might examine the interface formed on changing the growth voltage. Relationships do exist between microstructure and growth conditions, although the data in the present work were insufficient to give clear results. Evidence for variations of microstructure with concentration, applied voltage, fiber dimensions, and hydrogen evolution was found. In contrast to the other growths, the lowest-voltage (0.4 V) growth had a thick microstructure of the scale of the cellulose fibers. What physics determines the lower length scale at which growth is compact? The different dendrite forms need to be classified. It is interesting that all microstructures could on the 50-to 100-μm scale show branching. Branching is hence seen as an inherent feature of the growth at this scale, independent of microstructure. The wide variety of microstructure was a surprise to the investigators.

X-ray microanalysis of copper density did reveal scaling regimes on log-log plots. However, fractal interpretations of this scaling were unsatisfactory. In one case studied, the scaling regime seemed simply to be the variation of measured density, from a low magnification image with a few separated growths in the image, to a higher magnification image with a single growth in the image.

ACKNOWLEDGMENTS

This work would not have been possible without the good technical support available at Royal Halloway and Bedford New College. We would like to thank S. Richards, M. Draper, M. Solcombe, J. Turner, S. Janes, G. Lawes, and the electron microscope (EM) unit in this context, and Fotosparks of Reading. Useful discussions and comments were made by R. Ball, S. Murphy, D. Heyes, and H. Weigel. One of us (J.R.M.) thanks SERC for partial support.

*Present address: The Blackett Laboratory, Imperial College, London SW7 2B7, United Kingdom.

[1]R. M. Brady and R. C. Ball, Nature (London) **309**, 225 (1984).

[2]M. Matsushita, M. Sano, Y. Hayakawa, H. Honjo, and Y. Swada, Phys. Rev. Lett. **53**, 286 (1984).

[3]D. Grier, E. Ben-Jacob, R. Clarke, and L. M. Sander, Phys. Rev. Lett. **56**, 1264 (1986).

[4]Y. Swada, A. Doughterty, and J. P. Gollub, Phys. Rev. Lett. **56**, 1260 (1986).

[5]J. H. Kaufman, A. I. Nazzal, O. Melroy, and A. Kapitulnik, Phys. Rev. B **35**, 1881 (1987).

[6]B. B. Mandelbrot, *Fractal Geometry of Nature* (Freeman, San Francisco, 1982).

[7]*On Growth and Form*, edited by H. E. Stanely and N. Ostwesky (Martinus Nijhoff, 1986).

[8]J. S. Langer, Rev. Mod. Phys. **52**, 1 (1980).

[9]L. Patterson J. Fluid. Mech. **113**, 513 (1981); Phys. Rev. Lett. **52** 1621 (1984); L. Niemeyer, L. Pietronero, and A. J.

Wiesmann, *ibid.* **52,** 1033 (1984).
[10]G. Zweig and J. R. Whitaker, *Paper Chromatography and Electrophoresis* (Academic, New York, 1967), Vol. 1, Chaps. 1 and 8.
[11]J. O'M. Bockris and A. K. N. Reddy, *Modern Electrochemistry* (Plenum, New York, 1973), Vol. 2.
[12]D. B. Hibbert, H. Sugiarto, and A. C. Tseung, J. Chem. Soc. Faraday Trans. 1 **74,** 1973 (1978).
[13]R. C. Ball, in *On Growth and Form,* edited by H. E. Stanely and N. Ostwesky (Martinus Nijhoff, 1986).
[14]R. F. Voss, Phys. Scr. T **13,** 27 (1986).
[15]R. C. Ball, in *Fractals in Physics,* edited by L. Pietronero and E. Tosatti (Elsevier, New York, 1986).
[16]P. Meakin, Faraday Discuss. Chem. Soc. **83,** (1987).
[17]J. Nittmann and H. E. Stanely, Nature (London) **321,** 663 (1986).
[18]L. M. Sander, Sci. Am. **256,** 82 (1987).
[19]H. J. Pick, G. G, Storey, and T. B. Vaughan, Electrochim. Acta. **2,** 165 (1960).
[20]T. C. Halsey, Phys. Rev. A **35,** 3512 (1987).
[21]P. Meakin, Chem. Phys. Lett. **123,** 428 (1986).
[22]E. Be. Jacob, G. Deutscher, P. Graik, N. D. Goldenfeld, and Y. Lareah, Phys. Rev. Lett. **57,** 1903 (1986).
[23]S. Liang and L. P. Kadanoff, Phys. Rev. A **31,** 2628 (1985).
[24]Y. Sawada, in *Statphys 16,* edited by E. H. Stanely (North-Holland, Amsterdam, 1987), p. 134.
[25]These questions have been addressed recently by T. C. Halsey, Phys. Rev. A **36,** 3512 (1987); and D. G. Grier, D. A. Kessler, and L. M. Sander, Phys. Rev. Lett. **59,** 2315 (1987).

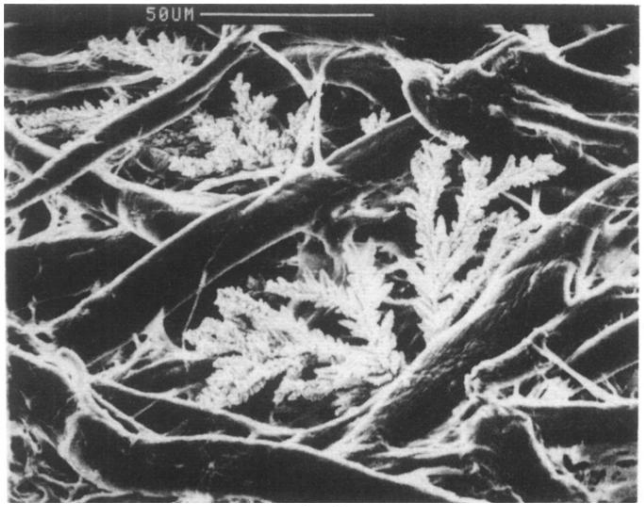

(a)

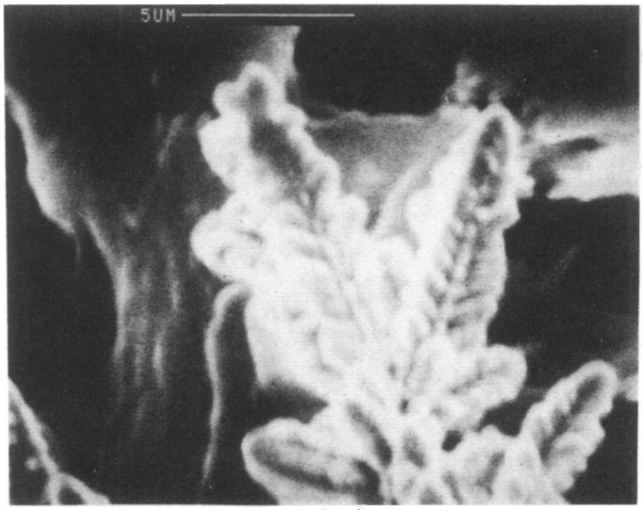

(b)

FIG. 10. A growth from 2-V, 0.75 mol dm^{-3} $CuSO_4$, 1 mol dm^{-3} H_2SO_4 solution. The dendrites of (b) are central to (a). Note the tip splitting on the left-hand finger.

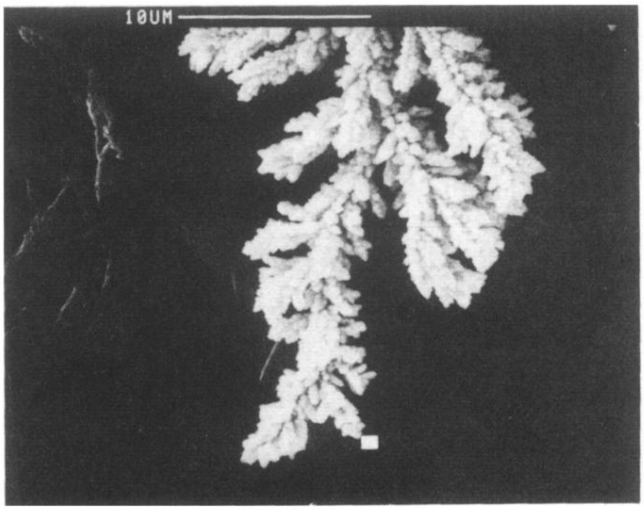

(a)

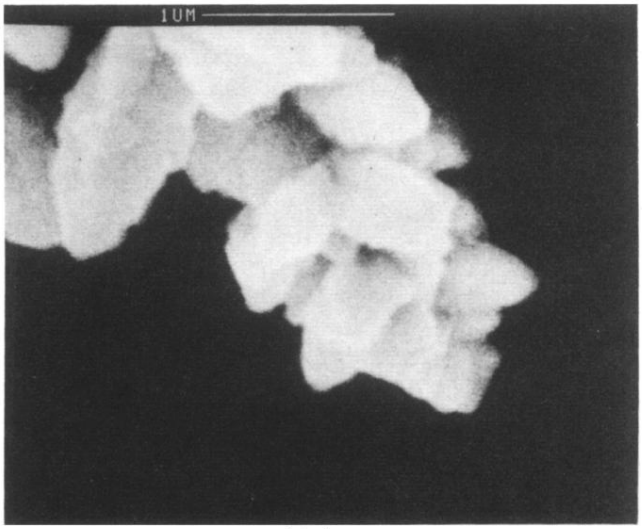

(b)

FIG. 11. A growth from 1 V, 0.5 mol dm^{-3} $CuSO_4$, 1 mol dm^{-3} H_2SO_4. The white square in (a) indicates the tip shown in (b).

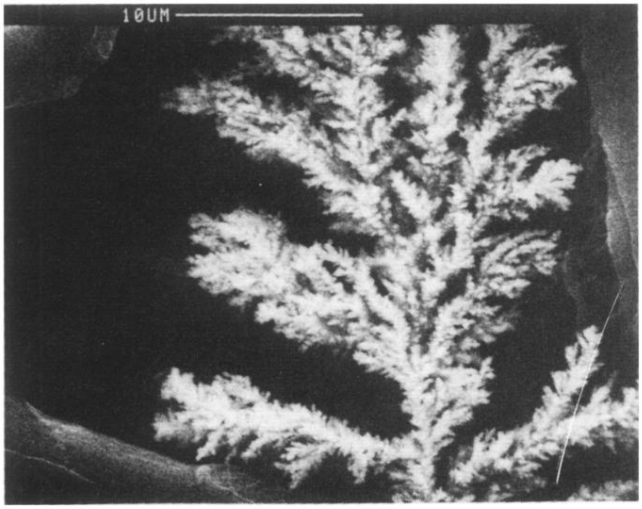

FIG. 12. A growth from 1 V, 0.1 mol dm^{-3} $CuSO_4$, 1 mol dm^{-3} H_2SO_4.

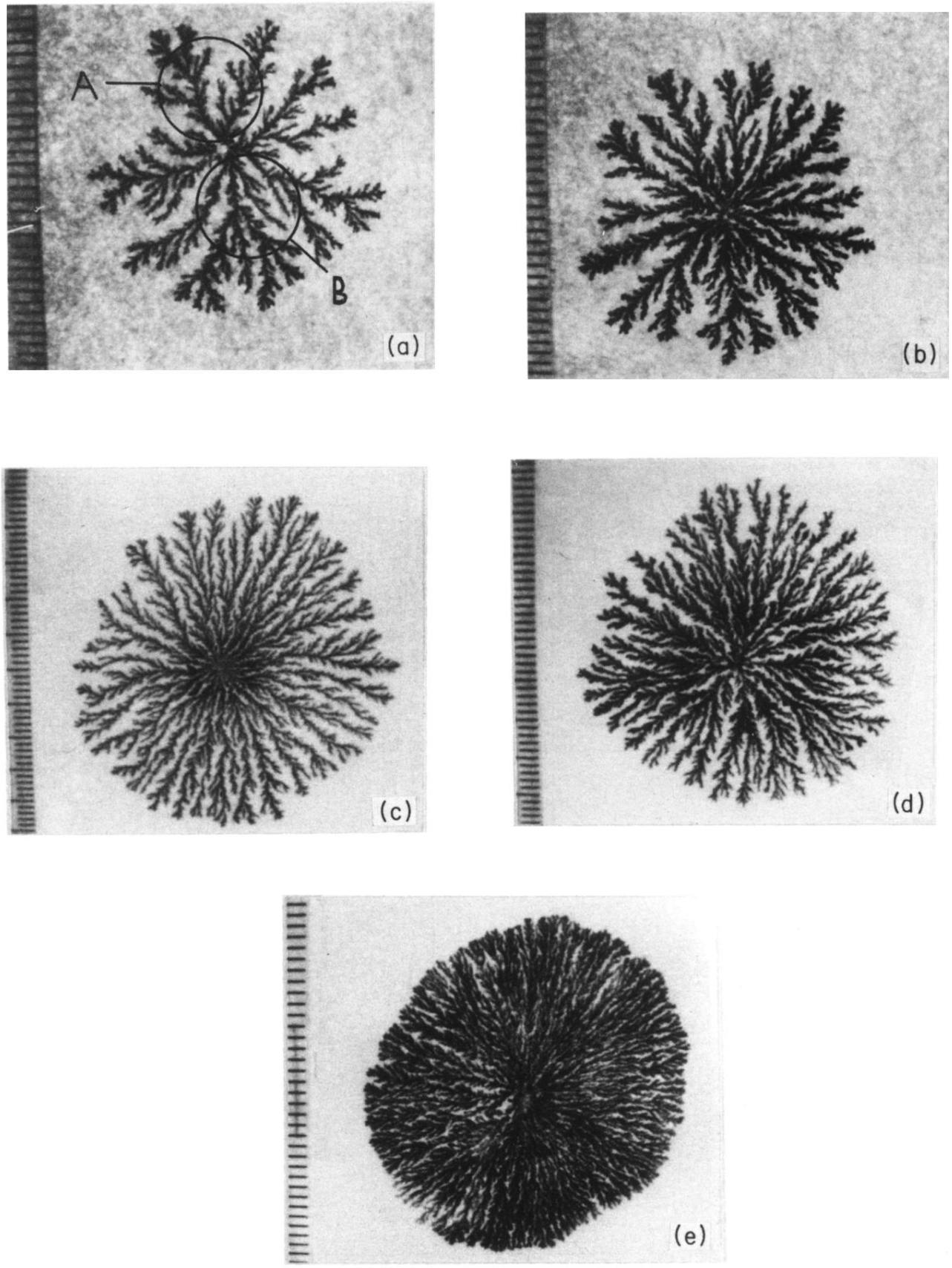

FIG. 2. Five samples grown potentiostatically from 0.75 mol dm^{-3} $CuSO_4$, 1 mol dm^{-3} H_2SO_4. (a) 0.5 V, d_f varying from 1.73 in region A to 1.91 in region B. (b) 0.7 V, $d_f = 1.79$. (c) 0.8 V, $d_f = 1.86$. (d) 1.6 V, $d_f = 1.95$. (e) 3 V, $d_f = 1.99$. A mm scale is shown.

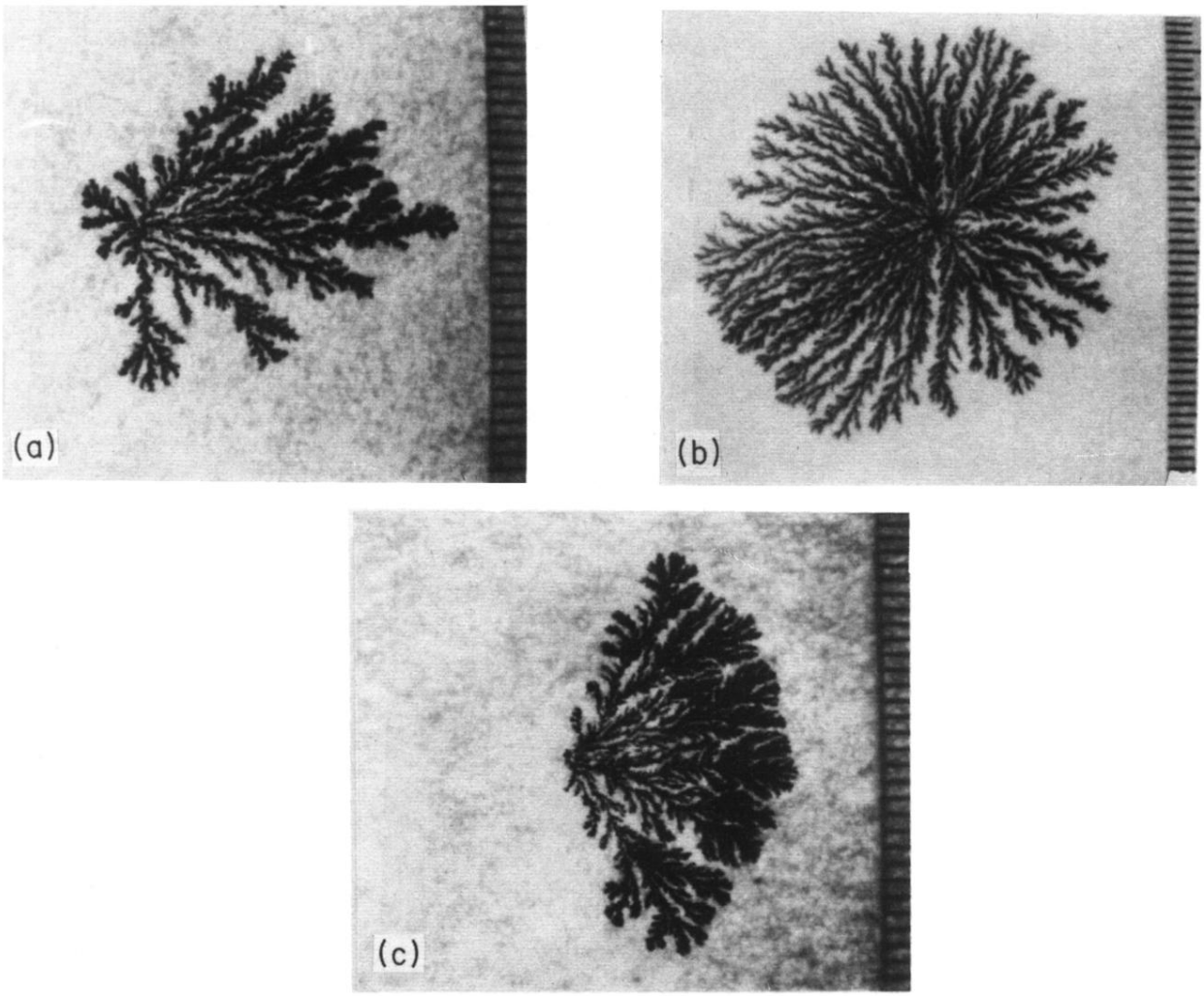

FIG. 4. Three samples showing anisotropic and inhomogeneous growth. (a) 1 V, (b) 1.4 V, and (c) 1 V. A mm scale is shown.

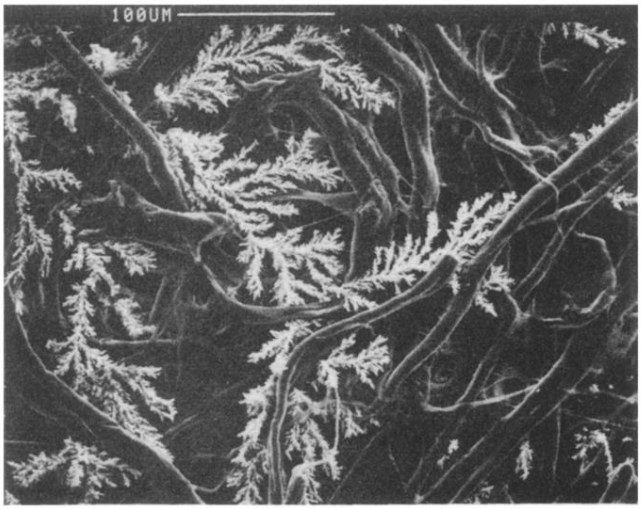

(a)

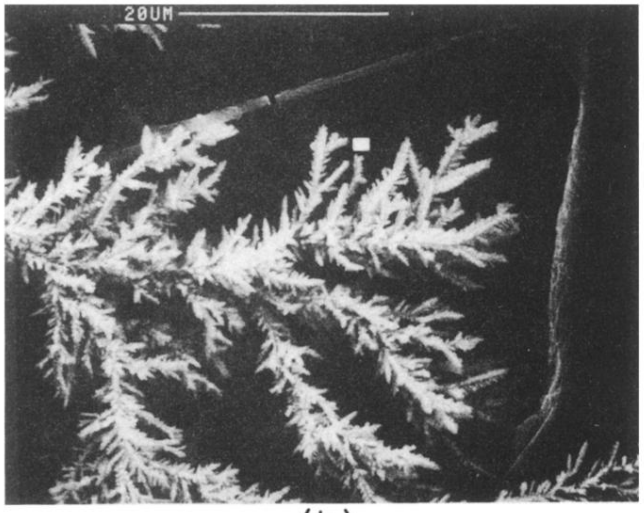

(b)

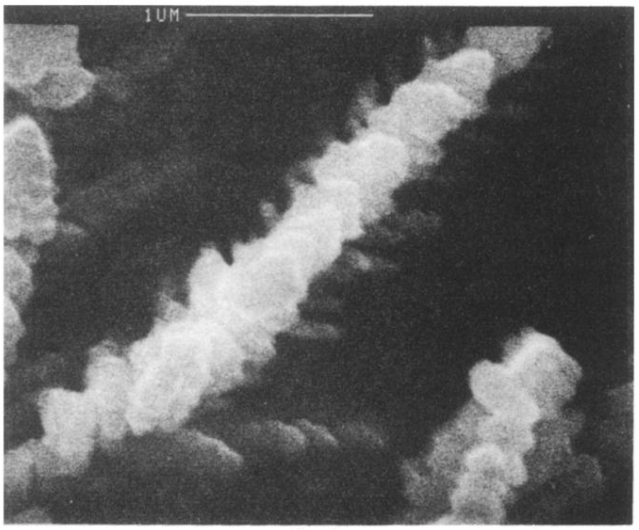

(c)

FIG. 6. Electron micrographs of the same region at three different magnifications from a growth at 1 V from a 0.25 mol dm^{-3} $CuSO_4$, 1 mol dm^{-3} H_2SO_4 solution. The growth in (a) is that which is central in (b). The white square in (b) indicates the dendrite shown in (c).

(a)

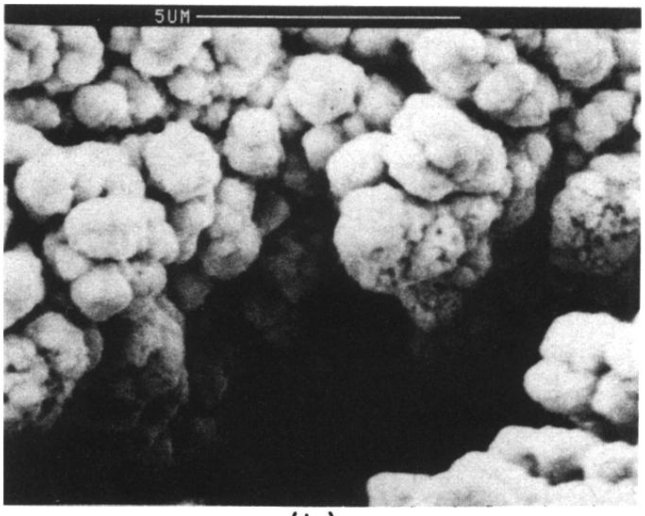

(b)

FIG. 7. The same region at two different magnifications from a growth at 2 V from 0.75 mol dm^{-3} $CuSO_4$, 1 mol dm^{-3} H_2SO_4. (b) is a close-up of the trough that is central on the growth of (a).

FIG. 8. A growth and fiber from a 3-V growth from 0.75 mol dm^{-3} $CuSO_4$, 1 mol dm^{-3} H_2SO_4. Note that the growth avoids the fiber surface.

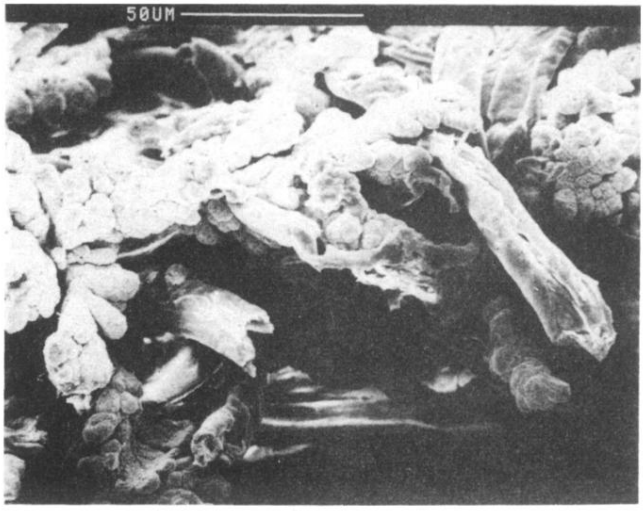

(a)

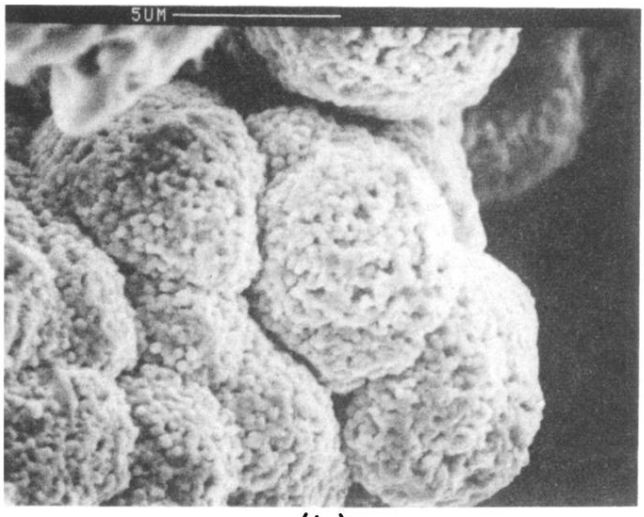

(b)

FIG. 9. Two different magnifications from 0.4 V, 0.75 mol dm^{-3} $CuSO_4$, 1 mol dm^{-3} H_2SO_4.